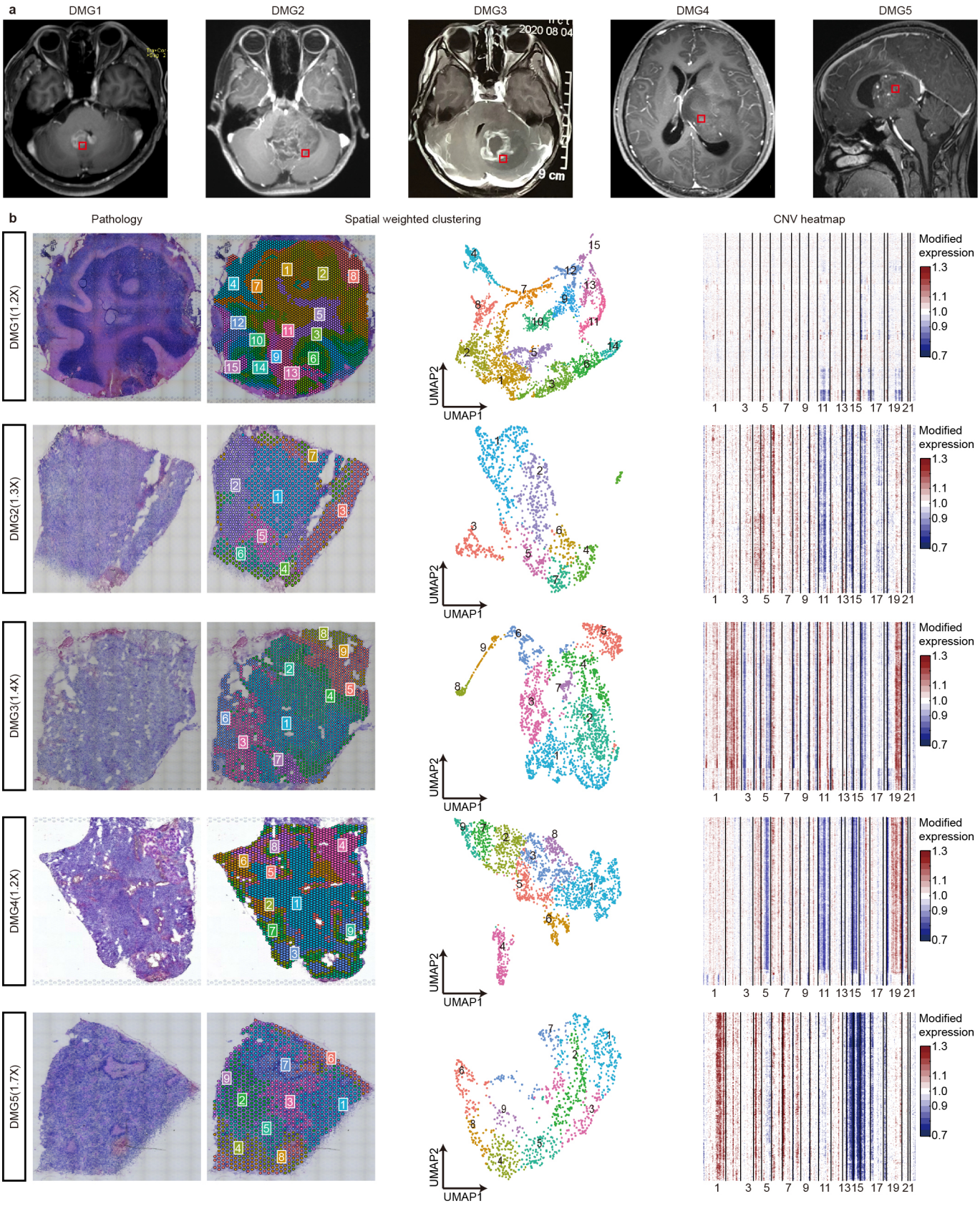
a
DMG1
DMG2
DMG3
DMG4
DMG5
2020 08 04
9 cm
b
Pathology
Spatial weighted clustering
CNV heatmap
DMG1(1.2X)
DMG2(1.3X)
DMG3(1.4X)
DMG4(1.2X)
DMG5(1.7X)
UMAP1
UMAP2
Modified expression
1.3
1.1
1.0
0.9
0.7
1 3 5 7 9 11 13 15 17 19 21
c
DMG1
DMG2
DMG3
DMG4
DMG5
H3K27M frequency
100%
50%
0

Supplementary Figure 1. MRI and spatial transcriptomic characterization of DMG samples.

a) Contrast-enhanced T1-weighted MRI images of DMG1-5 show the tumor locations. The sampling sites are marked by red boxes.

b) Left to right: H&E staining showing the histopathology, spatial/UMAP plots, and CNV heatmaps of DMG1-5. Spatial weighted clustering is based on BANKSY using default resolution parameters (0.8), visualized by Seurat. For CNV heatmaps, each row represents a spot and each column represents a chromosomal location. Red or blue represent chromosomal gain or loss, respectively.

c) H3K27M mutational frequency in spots from DMG1-5. Colors from white to red represent the ratio of wildtype or H3K27M-mutant reads, respectively. Transparent spots contain no reads detected at the H3K27 locus.

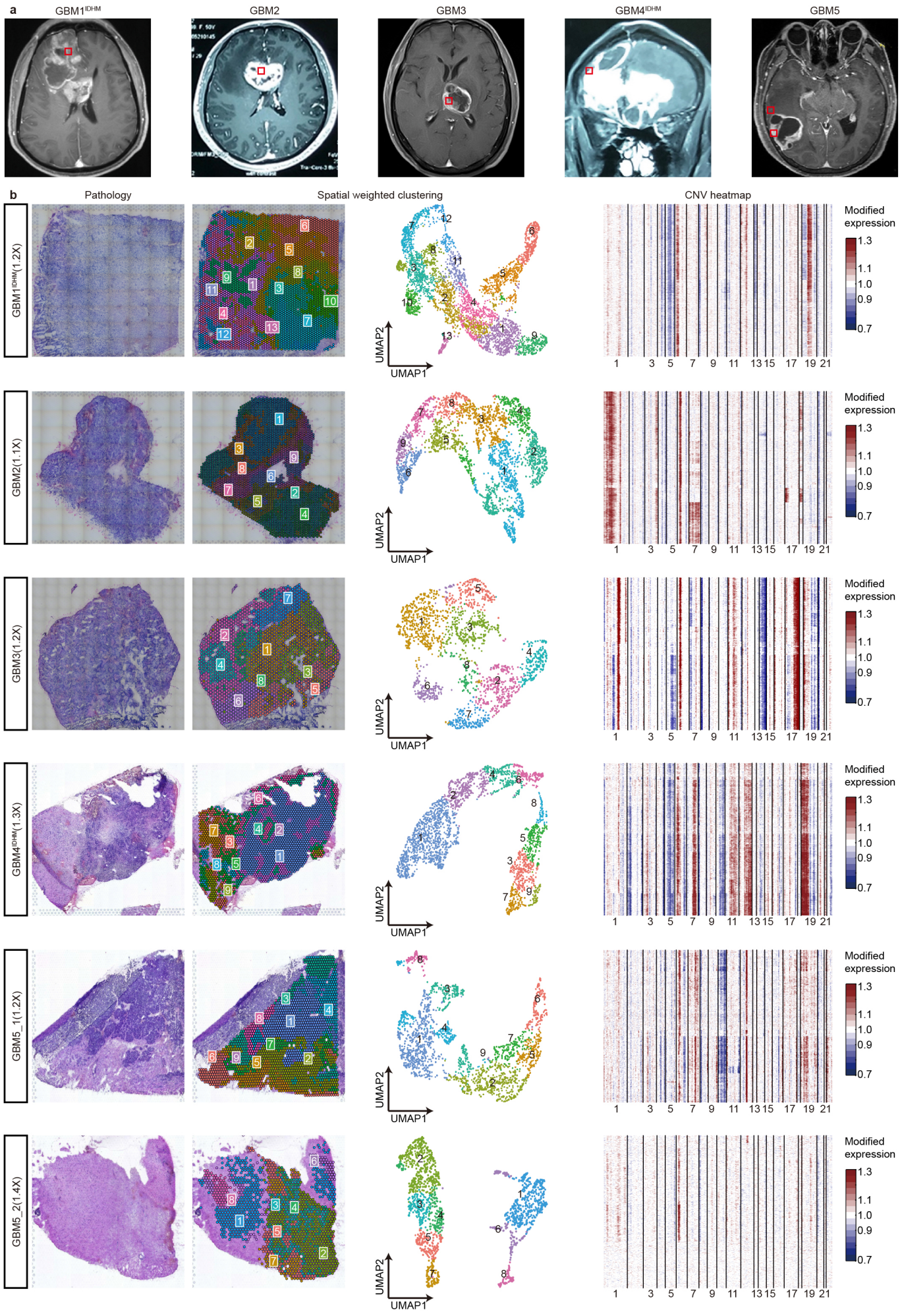
a
GBM1IDHM
GBM2
GBM3
GBM4IDHM
GBM5
b
Pathology
Spatial weighted clustering
CNV heatmap
GBM1IDHM(1.2X)
GBM2(1.1X)
GBM3(1.2X)
GBM4IDHM(1.3X)
GBM5_1(1.2X)
GBM5_2(1.4X)
UMAP1
UMAP2
Modified expression
1.3
1.1
1.0
0.9
0.7
1 3 5 7 9 11 13 15 17 19 21

Supplementary Figure 2. MRI and spatial transcriptomic characterization of GBM samples.

a) Contrast-enhanced T1-weighted MRI images of GBM1-5 show the tumor locations, The sampling sites are marked by red boxes (GBM5_1 and GBM5_2 were sampled from the same patient in the cortex and peritumor area, respectively).

b) Left to right: H&E staining showing the histopathology, spatial/UMAP plots, and CNV heatmaps of GBM1-5. Spatial weighted clustering is based on BANKSY using default resolution parameters (0.8), visualized by Seurat. For CNV heatmaps, each row represents a spot and each column represents a chromosomal location. Red or blue represent chromosomal gain or loss, respectively.

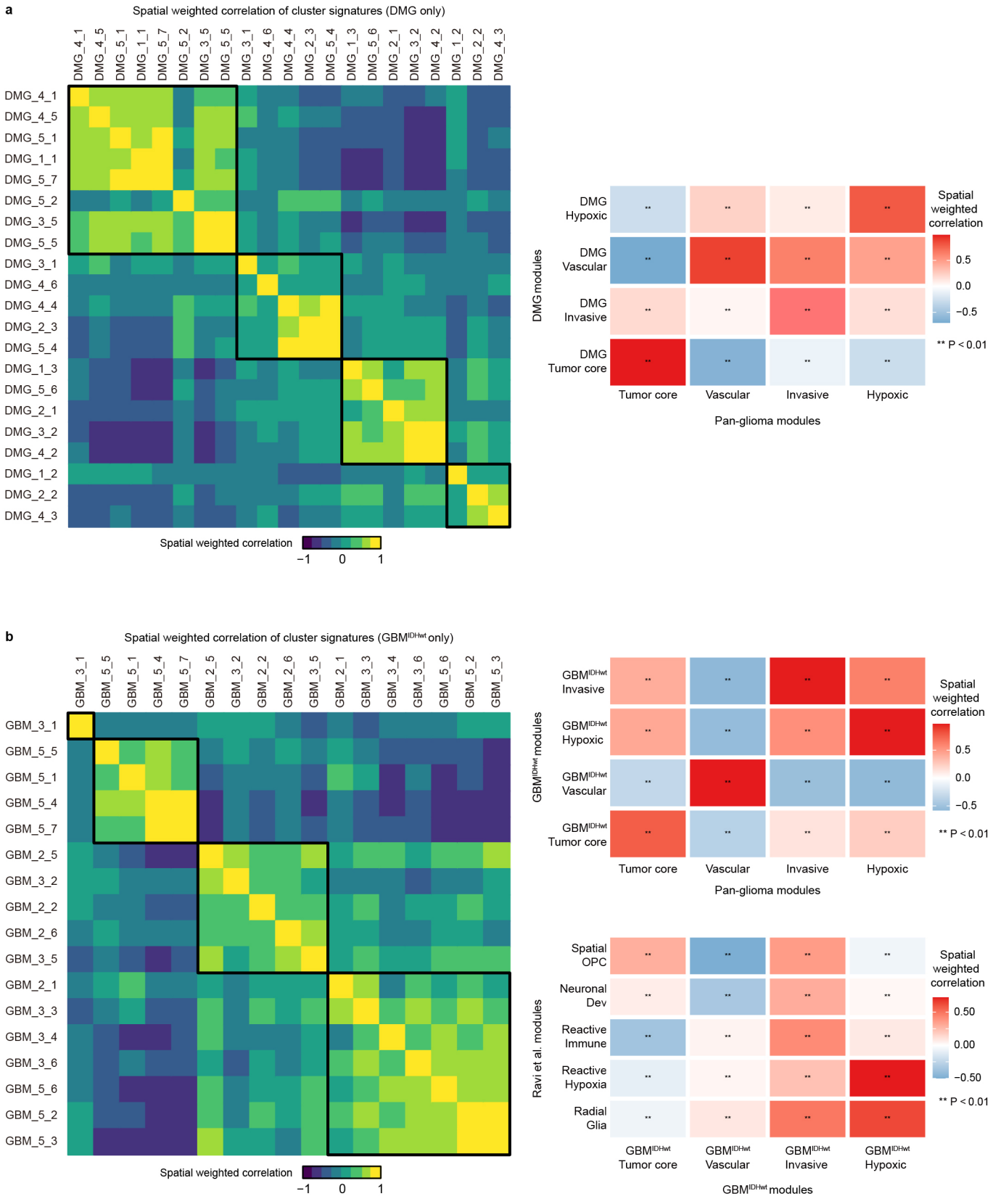
a
Spatial weighted correlation of cluster signatures (DMG only)
DMG_4_1
DMG_4_5
DMG_5_1
DMG_1_1
DMG_5_7
DMG_5_2
DMG_3_5
DMG_5_5
DMG_3_1
DMG_4_6
DMG_4_4
DMG_2_3
DMG_5_4
DMG_1_3
DMG_5_6
DMG_2_1
DMG_3_2
DMG_4_2
DMG_1_2
DMG_2_2
DMG_4_3
Spatial weighted correlation
−1
0
1
DMG modules
DMG Hypoxic
DMG Vascular
DMG Invasive
DMG Tumor core
Tumor core
Vascular
Invasive
Hypoxic
Pan-glioma modules
Spatial weighted correlation
0.5
0.0
−0.5
** P < 0.01
b
Spatial weighted correlation of cluster signatures (GBM^IDHwt only)
GBM_3_1
GBM_5_5
GBM_5_1
GBM_5_4
GBM_5_7
GBM_2_5
GBM_3_2
GBM_2_2
GBM_2_6
GBM_3_5
GBM_2_1
GBM_3_3
GBM_3_4
GBM_3_6
GBM_5_6
GBM_5_2
GBM_5_3
Spatial weighted correlation
−1
0
1
GBM^IDHwt modules
GBM^IDHwt Invasive
GBM^IDHwt Hypoxic
GBM^IDHwt Vascular
GBM^IDHwt Tumor core
Tumor core
Vascular
Invasive
Hypoxic
Pan-glioma modules
Spatial weighted correlation
0.5
0.0
−0.5
** P < 0.01
Ravi et al. modules
Spatial OPC
Neuronal Dev
Reactive Immune
Reactive Hypoxia
Radial Glia
GBM^IDHwt Tumor core
GBM^IDHwt Vascular
GBM^IDHwt Invasive
GBM^IDHwt Hypoxic
GBM^IDHwt modules
Spatial weighted correlation
0.50
0.00
−0.50
** P < 0.01

Supplementary Figure 3. Niche-specific spatial transcriptional programs by tumor types.

a) Left: Heatmap of spatially weighted correlation of the 21 spatial cluster signatures from five DMG samples. Hierarchical clustering confirmed 4 clustered programs. Spatial cluster information is marked on the top and left. Right: Heatmap of spatial weighted correlation between DMG modules and pan-glioma modules. Correlation and P values were determined by non-parametric Spearman's correlation test, Bonferroni-corrected for multiple comparisons. Source data are provided as a Source Data file, and individual P values are included.

b) Left: Heatmap of spatially weighted correlation of the 17 spatial cluster signatures from three $IDH^{wildtype}$ GBM samples. Hierarchical clustering confirmed 4 clustered programs. Spatial cluster information is marked on the top and left. Right: Top) Heatmap of spatial weighted correlation between $IDH^{wildtype}$ GBM modules and pan-glioma modules. Bottom) Heatmap of spatial weighted correlation between $IDH^{wildtype}$ GBM modules and Ravi et al. modules. Correlation and P values were determined by non-parametric Spearman's correlation test, Bonferroni-corrected for multiple comparisons. Source data are provided as a Source Data file, and individual P values are included.

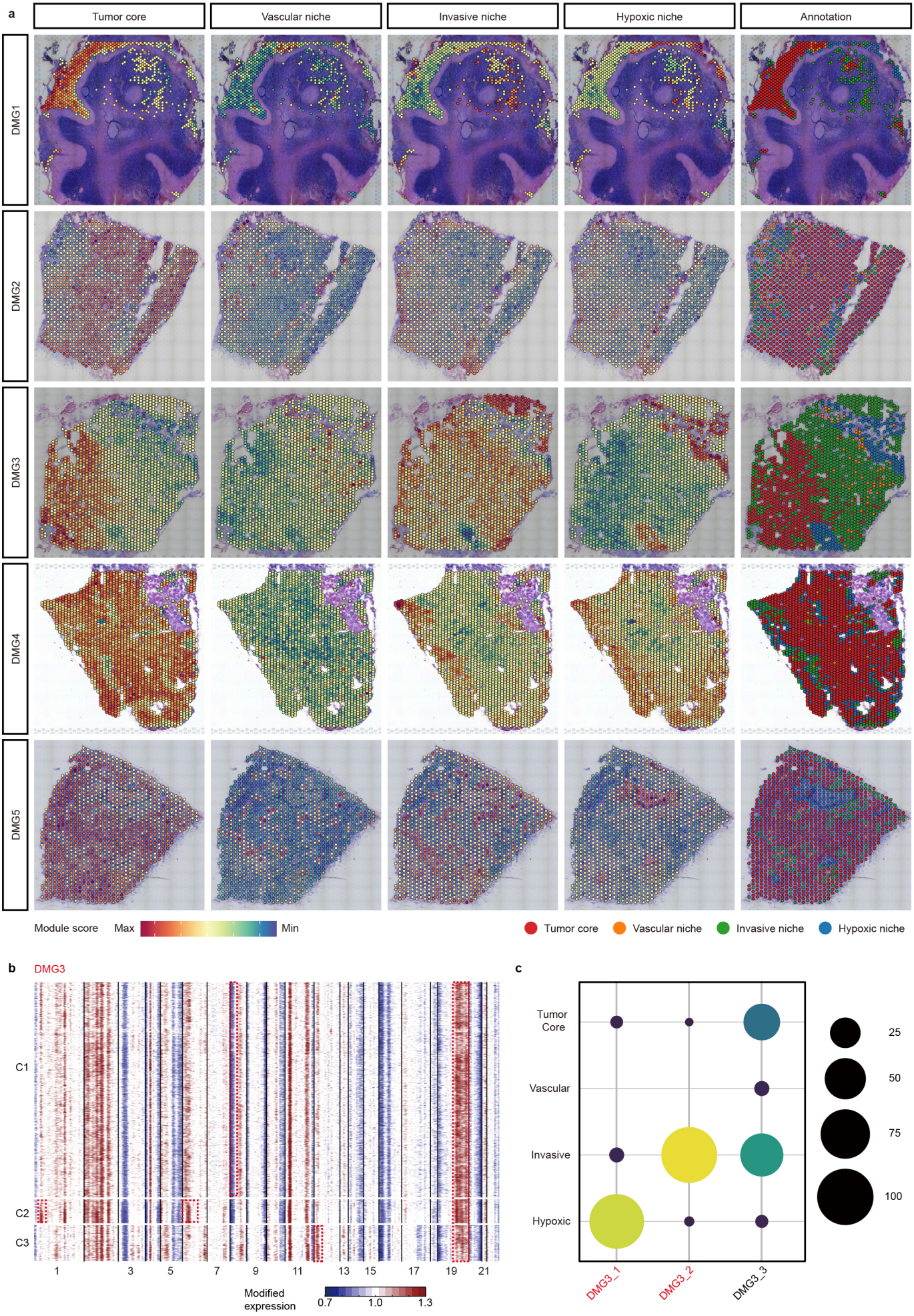
a
Tumor core
Vascular niche
Invasive niche
Hypoxic niche
Annotation
DMG1
DMG2
DMG3
DMG4
DMG5
Module score
Max
Min
Tumor core
Vascular niche
Invasive niche
Hypoxic niche
b
DMG3
C1
C2
C3
1
3
5
7
9
11
13
15
17
19
21
Modified expression
0.7
1.0
1.3
c
Tumor Core
Vascular
Invasive
Hypoxic
DMG3_1
DMG3_2
DMG3_3
25
50
75
100

Supplementary Figure 4. Niche-enriched spatial transcriptomic signatures and tumor subclones in DMG samples.

a) Left: scaled expression of Module scores 1-4 corresponding to niche identities in DMG1-5. Right: Each spot is assigned a niche identity based on their highest expressing module score, marked by different colors.

b) An example of subclone assignment based on prominent CNV events (dashed red boxes) in the InferCNV heatmap, showing 3 major subclones (C1-C3) from DMG3.

c) Dot plot indicating the spot distribution of subclones (columns) from DMG3 across different niches (rows). Dot size and color reflect the percentage. The niche-dominant subclones (>=75% in one niche) are highlighted in red.

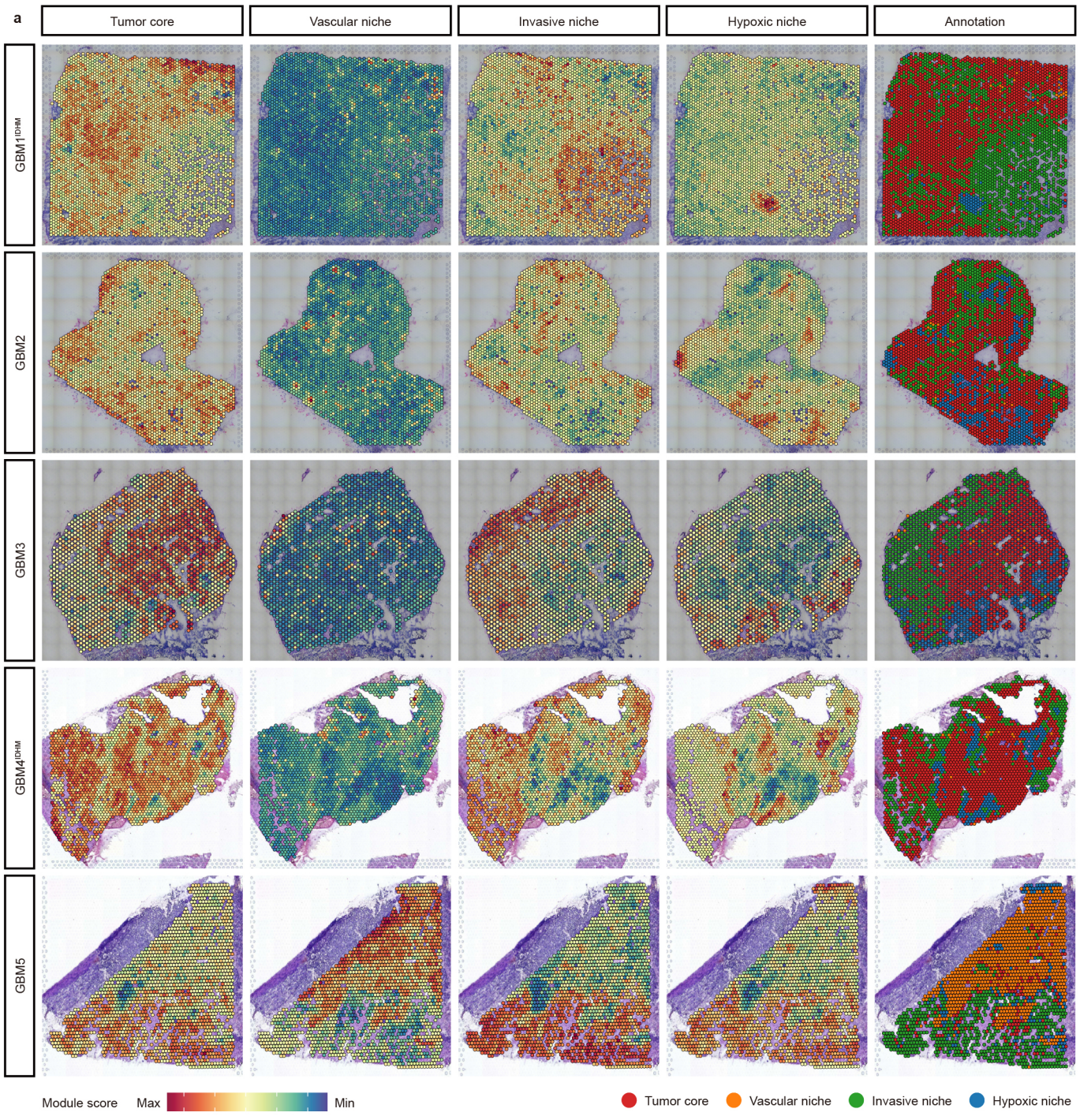
a
Tumor core
Vascular niche
Invasive niche
Hypoxic niche
Annotation
GBM1IDHM
GBM2
GBM3
GBM4IDHM
GBM5
Module score
Max
Min
Tumor core
Vascular niche
Invasive niche
Hypoxic niche
b
GBM2
C5
C4
C3
C2
C1
1
3
5
7
9
11
13
15
17
19
21
Modified expression
0.7
1.0
1.3
c
Tumor Core
Vascular
Invasive
Hypoxic
GBM2_1
GBM2_2
GBM2_3
GBM2_4
GBM2_5
25
50
75
100

Supplementary Figure 5. Niche-enriched spatial transcriptomic signatures and tumor subclones in DMG samples.

a) Left: scaled expression of Module scores 1-4 corresponding to niche identities in GBM1-5. Right: Each spot is assigned a niche identity based on their highest expressing module score, marked by different colors.

b) An example of subclone assignment based on prominent CNV events (dashed red boxes) in the InferCNV heatmap, showing 5 major subclones (C1-C5) from GBM2.

c) Dot plot indicating the spot distribution of subclones (columns) from DMG3 across different niches (rows). Dot size and color reflect the percentage. The niche-dominant subclone (>=75% in one niche) is highlighted in red.

a

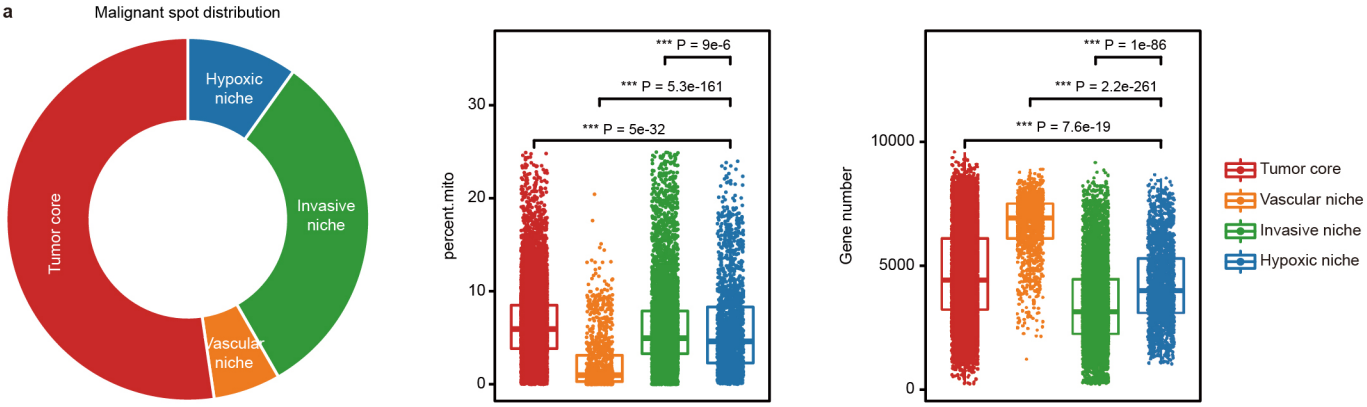
Malignant spot distribution
Hypoxic niche
Invasive niche
Vascular niche
Tumor core
percent.mito
*** P = 9e-6
*** P = 5.3e-161
*** P = 5e-32
Gene number
*** P = 1e-86
*** P = 2.2e-261
*** P = 7.6e-19
Tumor core
Vascular niche
Invasive niche
Hypoxic niche

b

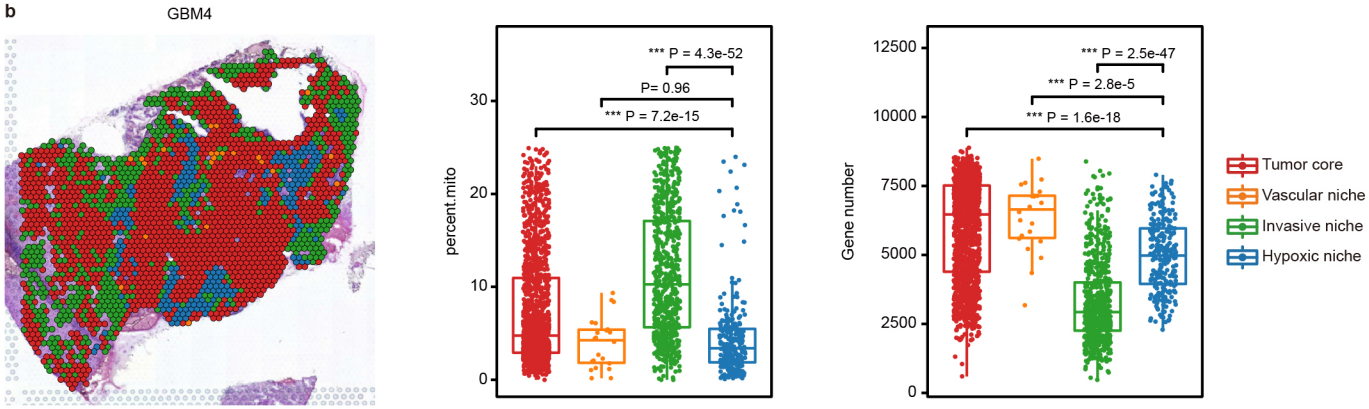
GBM4
percent.mito
*** P = 4.3e-52
P= 0.96
*** P = 7.2e-15
Gene number
*** P = 2.5e-47
*** P = 2.8e-5
*** P = 1.6e-18
Tumor core
Vascular niche
Invasive niche
Hypoxic niche

c

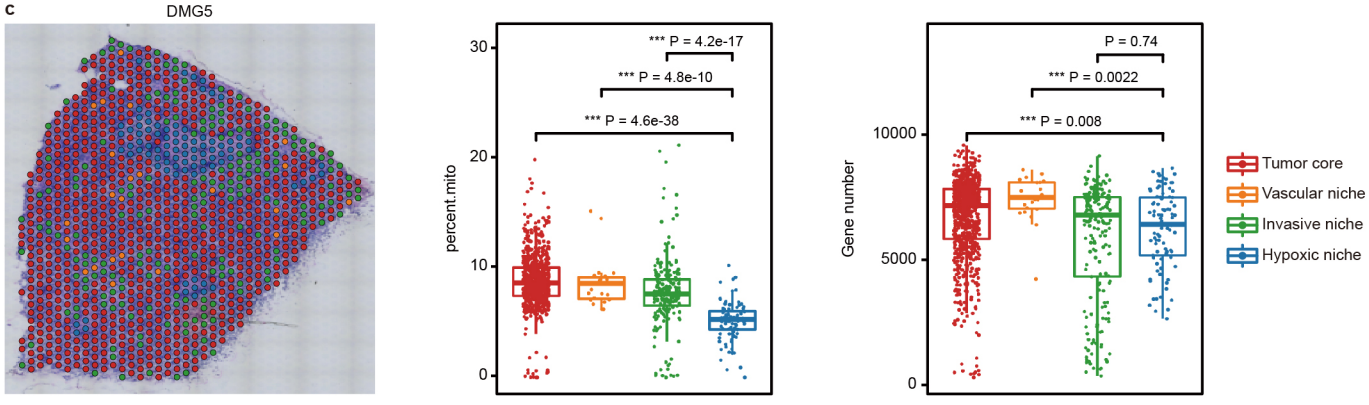
DMG5
percent.mito
*** P = 4.2e-17
*** P = 4.8e-10
*** P = 4.6e-38
Gene number
P = 0.74
*** P = 0.0022
*** P = 0.008
Tumor core
Vascular niche
Invasive niche
Hypoxic niche

Supplementary Figure 6. Quality control of malignant spots in different niches.

a) Left: Pie chart indicating the percentage of spots assigned to different niches. Right: Box plots of the percentage of mitochondrial genes and the total number of genes in each spot, grouped by niche identity (n = 10342, 1182, 6290, and 1951 spots, respectively). Boxes indicate quartiles, horizontal bar indicate median, and whiskers indicate range, up to 1.5-fold inter-quartile range. P values, Kruskal–Wallis test for differences between groups with Holm's correction for multiple comparisons.

b, c) Two examples of samples with prominent pseudopalisiding histopathology. Left: spatial plots of four niches for GBM4 (b) and DMG5 (c), distinguished by color. Right: Box plots of the percentage of mitochondrial genes and the total number of genes in each spot from GBM4 (n = 1447, 22, 645, and 249 spots, respectively) and DMG5 (n = 750, 23, 194, and 89 spots, respectively), grouped by niche identity. Boxes indicate quartiles, horizontal bar indicate median, and whiskers indicate range, up to 1.5-fold inter-quartile range. P values, Kruskal–Wallis test for differences between groups with Holm's correction for multiple comparisons.

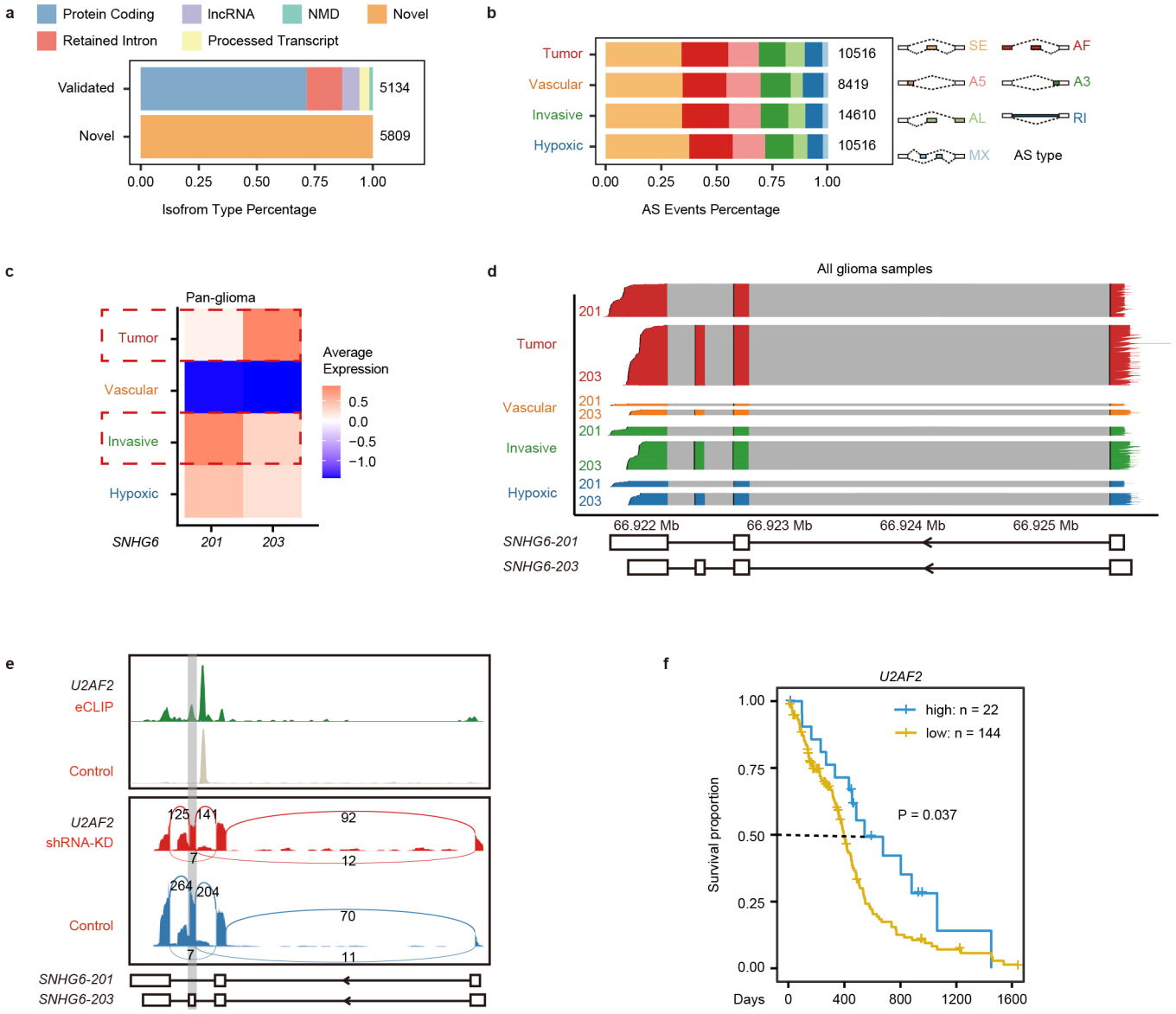
a
Protein Coding
lncRNA
NMD
Novel
Retained Intron
Processed Transcript
Validated
Novel
5134
5809
0.00
0.25
0.50
0.75
1.00
Isofrom Type Percentage
b
Tumor
Vascular
Invasive
Hypoxic
10516
8419
14610
10516
SE
AF
A5
A3
AL
RI
MX
AS type
0.00
0.25
0.50
0.75
1.00
AS Events Percentage
c
Pan-glioma
Tumor
Vascular
Invasive
Hypoxic
Average Expression
0.5
0.0
−0.5
−1.0
SNHG6
201
203
d
All glioma samples
Tumor
Vascular
Invasive
Hypoxic
201
203
66.922 Mb
66.923 Mb
66.924 Mb
66.925 Mb
SNHG6-201
SNHG6-203
e
U2AF2
eCLIP
Control
U2AF2
shRNA-KD
Control
125
141
92
7
12
264
204
70
7
11
SNHG6-201
SNHG6-203
f
U2AF2
high: n = 22
low: n = 144
P = 0.037
Survival proportion
1.00
0.75
0.50
0.25
0.00
Days
0
400
800
1200
1600

Supplementary Figure 7. RNA isoform diversity across glioma niches.

a) Bar plot of the percentages of isoform types. The total numbers of validated and novel isoforms are labeled. NMD, nonsense-mediated decay.

b) Bar plot of the percentages of AS types in different niches. The total numbers of AS events in each niche are labeled. SE, skipping exon. AF, alternative first exon. A5, alternative 5' splice-site. A3, alternative 3' splice-site. AL, alternative last exon. RI, retained intron. MX, mutually exclusive exons.

c, d) Differential isoform enrichment of *SNHG6-201* and *SNHG6-203* in different niches of all glioma samples (n= 19,071 spots), shown by tile plots (c) and individual transcripts in each niche (d).

e) Predicted splicing regulation of *SNHG6* by splicing factor *U2AF2*. Peaks indicate eCLIP and shRNA-KD RNA-seq read density in HepG2 cell line from ENCODE[37]. Biological replicates have similar results. Grey box shows the alternatively spliced region of *SNHG6-203.*

f) Kaplan–Meier survival curves comparing the overall survival between *U2AF2* high (n = 12) versus low groups (n = 144) in the TCGA GBM cohort[36]. Curve comparison P value was determined by two tailed Log-rank (Mantel-Cox) test.

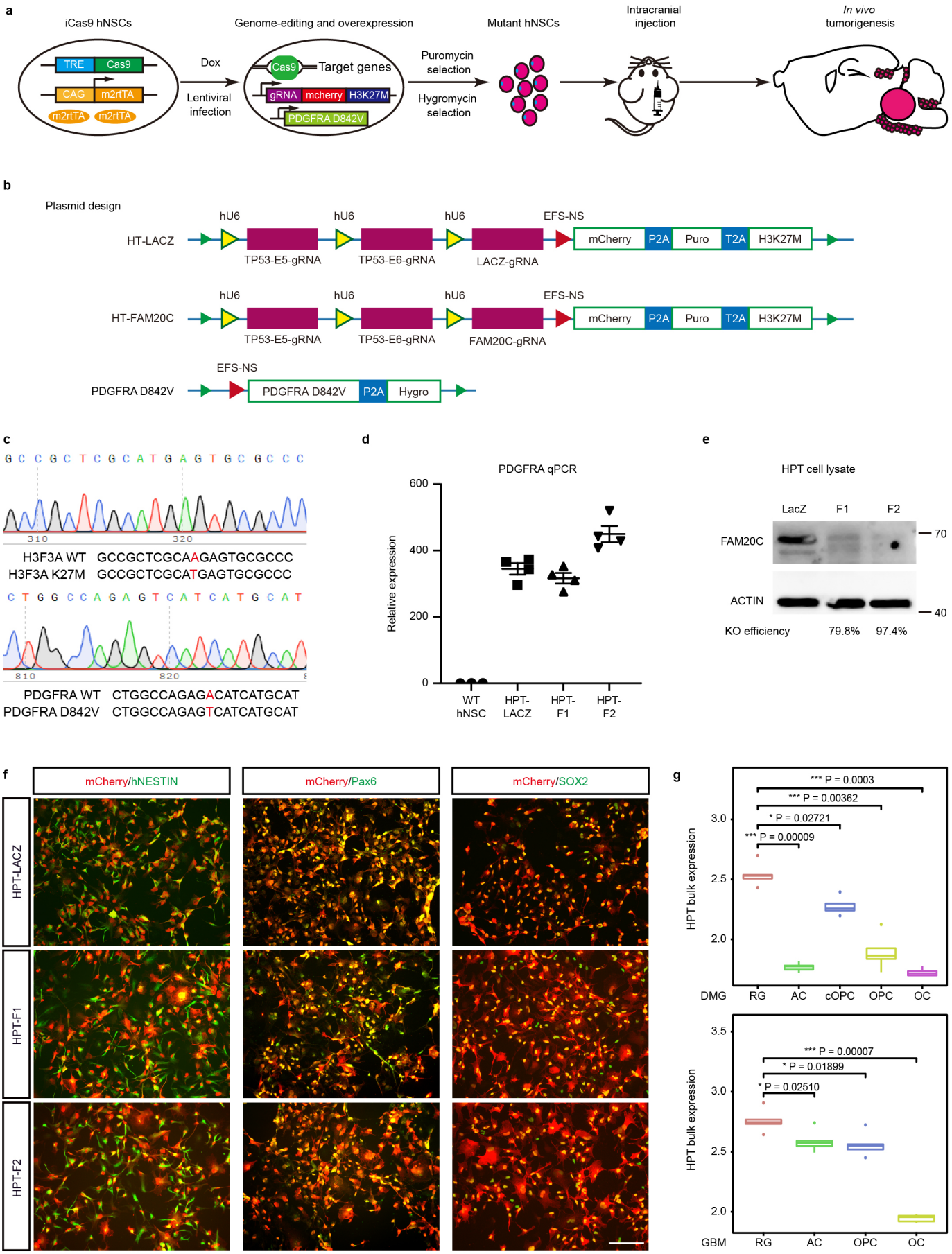
a
iCas9 hNSCs
TRE
Cas9
CAG
m2rtTA
m2rtTA
m2rtTA
Dox
Lentiviral infection
Genome-editing and overexpression
Cas9
Target genes
gRNA
mcherry
H3K27M
PDGFRA D842V
Puromycin selection
Hygromycin selection
Mutant hNSCs
Intracranial injection
In vivo tumorigenesis
b
Plasmid design
HT-LACZ
hU6
TP53-E5-gRNA
hU6
TP53-E6-gRNA
hU6
LACZ-gRNA
EFS-NS
mCherry
P2A
Puro
T2A
H3K27M
HT-FAM20C
hU6
TP53-E5-gRNA
hU6
TP53-E6-gRNA
hU6
FAM20C-gRNA
EFS-NS
mCherry
P2A
Puro
T2A
H3K27M
PDGFRA D842V
EFS-NS
PDGFRA D842V
P2A
Hygro
c
H3F3A WT GCCGCTCGCAAGAGTGCGCCC
H3F3A K27M GCCGCTCGCATGAGTGCGCCC
PDGFRA WT CTGGCCAGAGACATCATGCAT
PDGFRA D842V CTGGCCAGAGTCATCATGCAT
d
PDGFRA qPCR
Relative expression
600
400
200
0
WT hNSC
HPT-LACZ
HPT-F1
HPT-F2
e
HPT cell lysate
LacZ
F1
F2
FAM20C
ACTIN
70
40
KO efficiency
79.8%
97.4%
f
mCherry/hNESTIN
mCherry/Pax6
mCherry/SOX2
HPT-LACZ
HPT-F1
HPT-F2
g
HPT bulk expression
*** P = 0.0003
*** P = 0.00362
* P = 0.02721
*** P = 0.00009
DMG
RG
AC
cOPC
OPC
OC
HPT bulk expression
*** P = 0.00007
* P = 0.01899
* P = 0.02510
GBM
RG
AC
OPC
OC

Supplementary Figure 8. Establishment and characterization of DMG-initiating HPT NSCs.

a) Workflow to generate DMG models from iCas9 hNSCs.

b) Design of HT-LACZ, HT-FAM20C, and PDGFRA D842V plasmids. sgRNAs targeting *TP53*, *LacZ*, *FAM20C* are driven by independent hU6 promoters. Overexpression of *H3K27M* and *PDGFRA D842V* is driven by EFs-NS promoters. mCherry is used as a reporter. Puromycin (Puro) and Hygromycin (Hygro) resistant transgenes are used for screening. P2A sequences encode self-cleave peptides to separate translated proteins encoded by different transgenes.

c) Sanger sequencing for *H3K27* and *PDGFRA* D842 locus in the constructed plasmids. Mutations are highlighted in red.

d) qPCR quantifying *PDGFRA* expression in WT, HPT-LACZ, HPT-F1, and HPT-F2 hNSCs. The qPCR experiment was repeated three times. Source data are provided as a Source Data file.

e) Western Blot analysis for FAM20C protein expression in HPT-LACZ, HPT_F1, and HPT-F2 hNSCs. β-ACTIN were used as loading controls. The knockout efficiency in HPT_F1 and HPT-F2 versus HPT-LACZ is calculated by comparing FAM20C band intensity normalized by β-ACTIN band intensity. The WB experiment was repeated three times. Source data are provided as a Source Data file.

f) Representative images of $mCherry^+$ HPT-LACZ, F1, or F2 cells (n = 3 for each group) stained with hNESTIN, PAX6, and SOX2. Scale bar, 200 μm.

g) The relative expression of cell-type specific gene sets (derived from DMG or GBM scRNAseq) in HPT-LACZ hNSCs were compared, based on bulk RNA-seq of HPT-LACZ hNSCs (n = 5). Boxes indicate quartiles, horizontal bar indicate median, and whiskers indicate range, up to 1.5-fold inter-quartile range. P values, Kruskal–Wallis test for between group differences with Benjamini–Hochberg's correction for multiple comparisons.

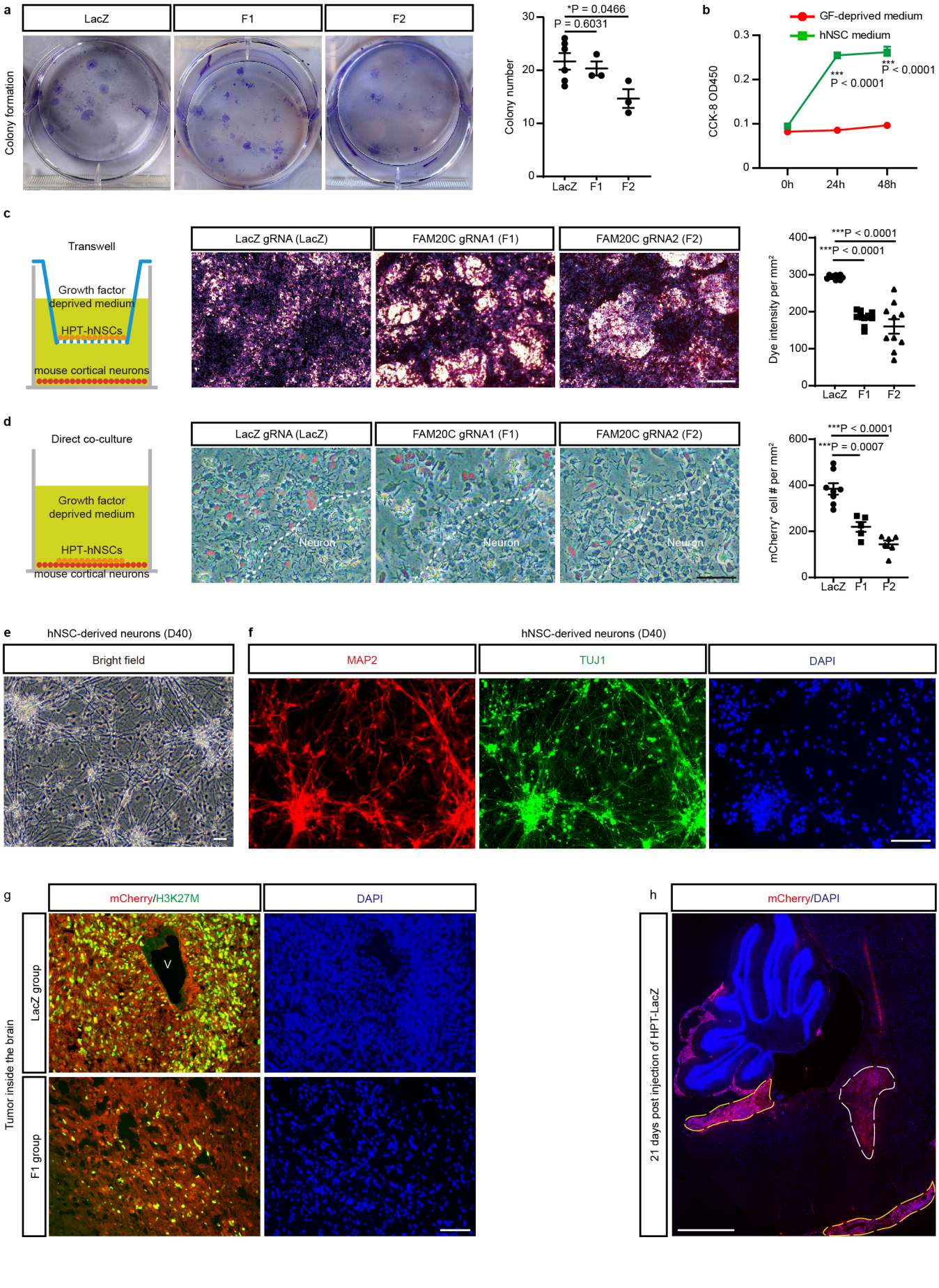
a
LacZ
F1
F2
Colony formation
*P = 0.0466
P = 0.6031
Colony number
30
20
10
0
LacZ F1 F2
b
GF-deprived medium
hNSC medium
CCK-8 OD450
0.3
0.2
0.1
0
***
P < 0.0001
***
P < 0.0001
0h 24h 48h
c
Transwell
Growth factor deprived medium
HPT-hNSCs
mouse cortical neurons
LacZ gRNA (LacZ)
FAM20C gRNA1 (F1)
FAM20C gRNA2 (F2)
***P < 0.0001
***P < 0.0001
Dye intensity per mm²
400
300
200
100
0
LacZ F1 F2
d
Direct co-culture
Growth factor deprived medium
HPT-hNSCs
mouse cortical neurons
LacZ gRNA (LacZ)
FAM20C gRNA1 (F1)
FAM20C gRNA2 (F2)
Neuron
Neuron
Neuron
***P < 0.0001
***P = 0.0007
mCherry⁺ cell # per mm²
600
400
200
0
LacZ F1 F2
e
hNSC-derived neurons (D40)
Bright field
f
hNSC-derived neurons (D40)
MAP2
TUJ1
DAPI
g
mCherry/H3K27M
DAPI
Tumor inside the brain
LacZ group
F1 group
V
h
mCherry/DAPI
21 days post injection of HPT-LacZ

Supplementary Figure 9. FAM20C promotes invasive growth of RG-like cells towards neurons.

a) Left: Representative images of colony formation assay for LacZ (n = 6), F1 (n = 3), and F2 (n = 3) HPT-hNSCs. Right: quantification for the total number of colonies. Scale bar, 1 cm. P values were determined by Student t-test. Error bars indicate mean ± SEM.

b) Cell proliferation was measured by CCK-8 assay. The growth curves of HPT-hNSCs cultured in normal or growth factor deprived hNSC culture medium from 0h to 48h are compared (n = 3 for each group at different time points). P values were determined by Student t-test. Error bars indicate mean ± SEM.

c) Left: Illustration of transwell assay with HPT-hNSCs in the top well and mouse cortical neurons in the bottom well in growth factor deprived medium. Middle: Representative images of crest violet staining for migrated LacZ, F1, and F2 HPT-hNSCs (n = 10 for each group). Right: Quantification of dye intensity per mm^2 membrane for each group. P values were determined by Student t-test. Error bars indicate mean ± SEM. Scale bar, 200 μm.

d) Left: Illustration of direct co-culture of HPT-hNSCs with mouse cortical neurons in growth factor deprived medium. Middle: Representative images of $mCherry^+$ LacZ (n = 8), F1 (n = 5), and F2 (n = 6) HPT-hNSCs adjacent to high-density neuronal clusters. Right: Quantification of the density of $mCherry^+$ HPT-hNSCs adjacent to high-density neuronal clusters for each group. P values were determined by Student t-test. Error bars indicate mean ± SEM. Scale bar, 200 μm.

e, f) Representative images of neurons differentiated from hNSCs at Day 40, bright field (e) (n = 3) or immunostained for MAP2/TUJ1/DAPI (f) (n = 3). Scale bars, 50 μm in e and 200 μm in f.

g) Representative images of IF co-labeling of mCherry/H3K27M for tumor areas inside the brains of LacZ and F1 groups (n = 10 for each group). V, blood vessel. Scale bar, 50 μm.

h) A representative image showing the distribution of $mCherry^+$ cells in the hindbrain 21 days post injection of HPT-LacZ hNSCs (n = 4). Scale bar, 1 mm.

Source data for a-d are provided as a Source Data file.